Design of vertical loaded raked steel piles

S. Höhmann
University of Applied Science, Holzminden, Germany

ABSTRACT: Deformations of the subsoil behind back-anchored structures of civil engineering result from various aspects such as consolidation due to load and subsoil compaction from the insertion of foundation piles with high energy. For the additional stresses on the anchoring element resulting from the deformations, there are currently no generally valid and adequate calculation models. The complex interaction of soil stratification, load, pile type and pile inclination, as well as the construction process, is only recorded realistically to a limited extent and is therefore not sufficiently taken into account in the known calculation approaches. Particularly in the case of large settlements, the approaches, which are usually based on elastic load-bearing behaviour, fail and thus lead to uneconomical cross-sections if used consistently. As a result of this lack of knowledge about the interaction between the soil and the pile, it is now controversial to what extent reinforcing the piles, the pile connections or changing the pile type sufficiently counteracts the problem. The present report attempts to describe the influencing variables and to transfer them to the boundary conditions of rammed steel piles and grouted anchors.

1 INTRODUCTION

Engineering structures, such as bank reinforcements and bridge abutments, are often designed as anchored structures. In this process, the backfill sands are often applied directly to existing cohesive soil layers. However, the consolidation that begins with the load inevitably leads to subsidence that forcibly deforms the previously introduced anchor elements like raked piles. The resulting increase in the anchor normal forces has already led to a failure of the anchor connection in some cases. Figure 1 is showing an example of a failed steel strap on the construction site in the port of Lübeck/Germany.

As a result of the settlement, deflections of the anchor element occur and thus additional stresses in the steel cross-section. However, inclinometer measurements also show corresponding deformations at the inclined pile in the case of filled non-cohesive soil layers (Gattermann 1999). Some examples of forced deformations are consolidation settlements, soil deformations from the filling process (ex. dredging material), compaction settlements of an installation process of driven piles and soil deformations from sheet pile deflection.

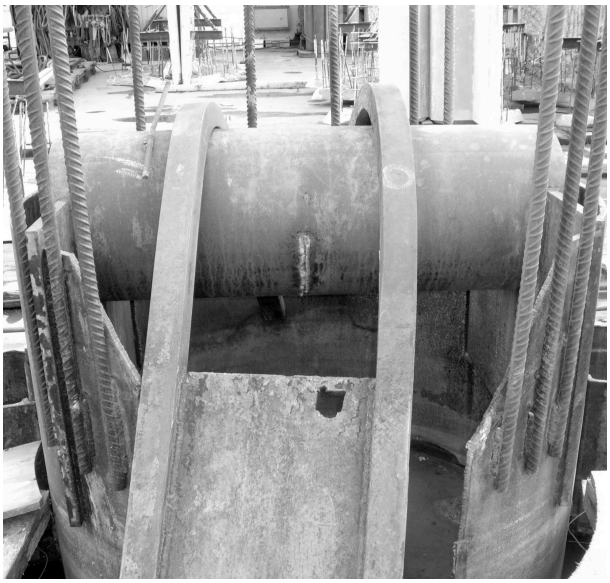

Figure 1. Failure of steel pile connection (right steel strap)

In addition to sufficient load-bearing capacity, the durability of the tie-back must also be ensured, taking into account the additional stresses.

Figure 2 shows an example of a vertical deformed inclined pile as a result of backfilling work with consolidation settlements of soft soils.

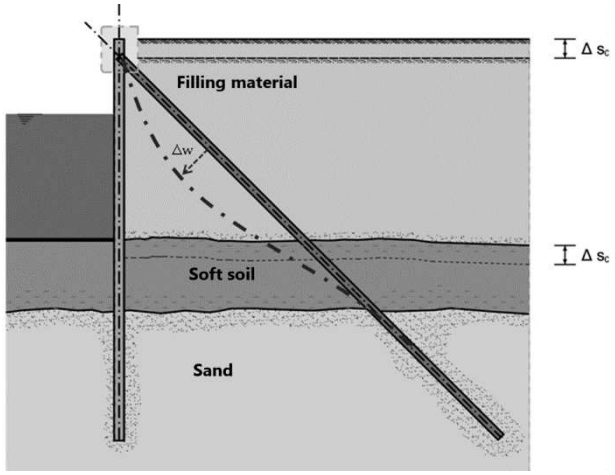

Figure 2. Vertical deformed inclined pile due to consolidation settlements

2 SETTLEMENTS

2.1 *General*

The settlement behaviour of non-cohesive soils is largely limited to a change in shape, which can be traced back to the rearrangement of the individual soil particles under load. These occur shortly after the load is applied and are therefore to be assigned to the immediate settlements. Elastic compressions of non-cohesive soils can usually be neglected as they are relatively small. However, compaction of loosely bedded sands can have a significant influence on the oblique loading of anchors.

The behaviour of cohesive soils under vertical loads varies from those of most granular soils as previously described. The settlement behaviour of cohesive materials is typically divided into three components (Fig. 3).

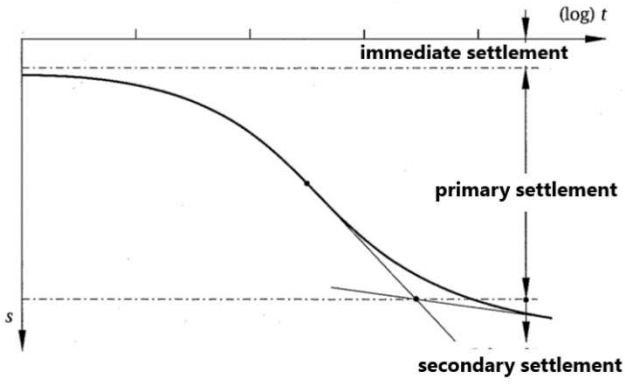

Figure 3. Time-settlement diagram according (Terzaghi 1943)

During immediate settlements taking place within a soil profile dominated by cohesive material, soil volumes remain largely unchanged. However, during consolidation the consolidation a large change in volume can take place as pore water is squeezed from the soil skeleton/grain structure with time (Knappett & Craig 2020). The final secondary settlements (creep settlements) are usually negligible in the context of settlement bending and are not described further here.

2.2 *Primary settlements*

The final or immediate settlement within a layer thickness Δh can be easily estimated with the help of the stiffness modulus $E_{s,k}$:

$$s_0 = \frac{1}{E_{s,k}} \int_0^h \sigma_z' \, dz = \frac{\sigma'_z}{E_{s,k}} \cdot h \qquad (1)$$

The stiffness modulus $E_{s,k}$ is determined in the laboratory as a secant modulus from oedometer tests. If no results from oedometer tests are available, the stiffness modulus can also be determined with the help of empirical approaches (Smoltczyk 2002).

2.3 *Compaction settlements*

The grains of these introduced non-cohesive soils will rearrange themselves in the further period due to vibration influences, such as when inserting foundation piles, and will take on a higher storage density. In addition, a different water level due to tidal influence can lead to a cyclical wall movement, which causes the soil to compact in the immediate vicinity (EAU 2020).

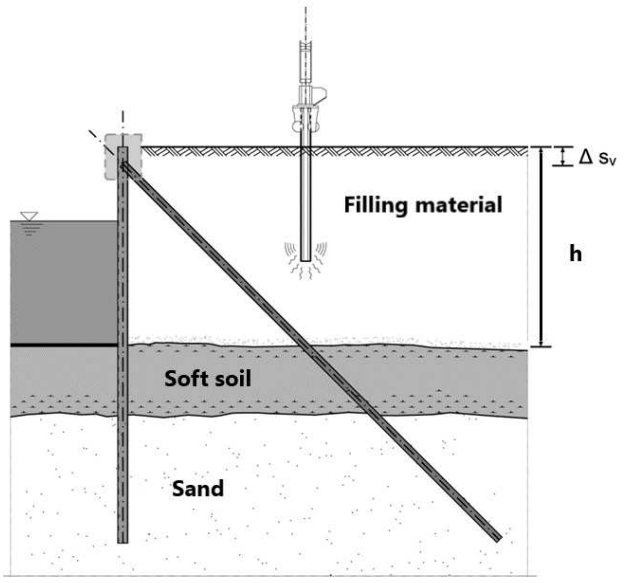

Figure 4. Lateral deformed inclined pile due to compaction settlements

The reduction of pore spaces tends to significant settlements. To determine the settlement size, the change in density D can be used as a simplified basis. During the present study the pore proportions of loosest storage n_{max} and densest storage n_{min} were to be determined.

On the basis of the information given above, the compaction s_V by the approach of changing the pore fraction from the initial state n_1 to the final state n_2 can be determined as follows

$$s_V = h \cdot (n_1 - n_2) \quad (2)$$

$$s_V = h \cdot (D_2 - D_1) \cdot (n_{max} - n_{min}) \quad (3)$$

where h = thickness of the filling material; n = porosity; and D = Density.

3 KNOWN CALCULATION APPROACHES

3.1 *General*

The filling of sands on cohesive layers inevitably results in soil movement transverse to the axial direction of the inclined pile. The magnitude of the impact depends on the subsoil stratification, the soil movement speed and the pile stiffness. In principle, a distinction must be made between an occurring flow pressure $p_{f,k}$ in the cohesive layers and a resulting earth pressure Δe_k

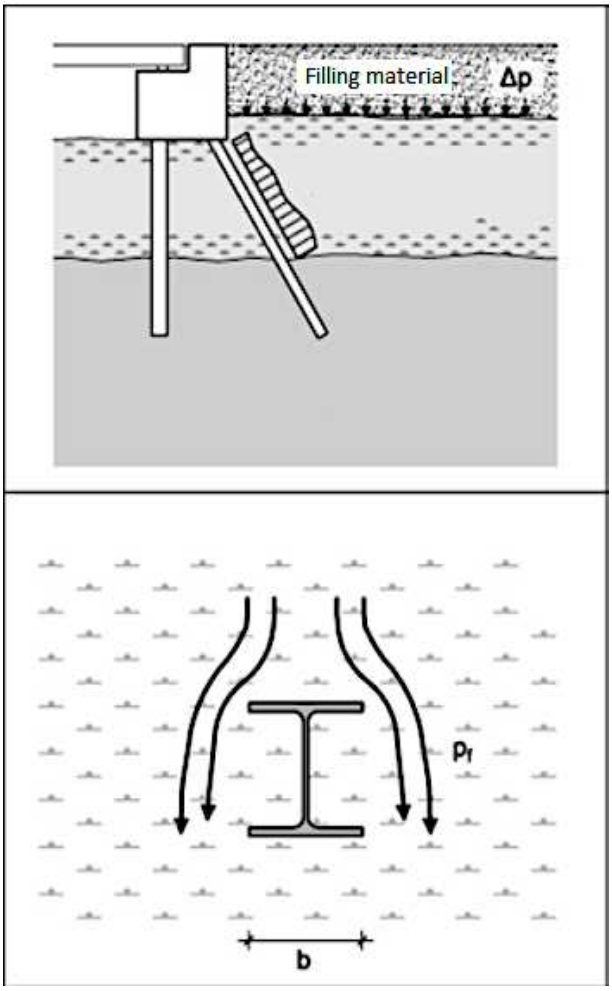

Figure 5. Possible flow pressure load on raked piles

The magnitude of the flow pressure has not yet been fully researched and can be determined as follows

$$p_{f,k} = f \cdot c_{u,k} \cdot b \quad (4)$$

The size factor f is referred to differently in the literature. The magnitude of the undrained shear strength $c_{u,k}$ is independent of the applied stresses and can usually be determined from an undrained triaxial test or from wing shear tests.

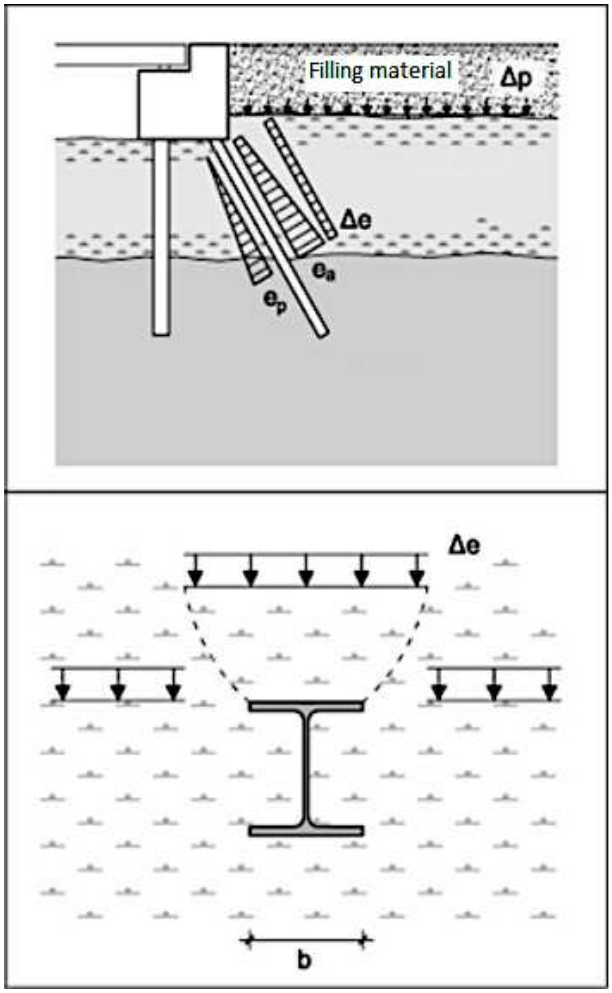

Figure 6. Possible earth pressure load on raked piles

According to EA-Pfähle (2013), the earth pressure acting on the pile Δe_k is calculated from the difference in earth pressures on the side of the pile facing the load or side facing away from the load. The decisive factor here is the range of loads.

3.2 *Analylize examples*

De Beer & Wallays (1972) developed two different loading approaches, which are applied depending on the safety of the slope fracture. In contrast to the approach shown above, the magnitude of the flow pressure depends on the load. If the safety in the slip circle is higher than η = 1.6, the load $p_{f,k}$ is applied constantly above the height of the soft layer in the event of a filled embankment.

In the case of less safety in the sliding circle than η = 1.6, two pairs of opposing loads limited in the sliding joint act on the pile. The doweling effect of the piles is not taken into account.

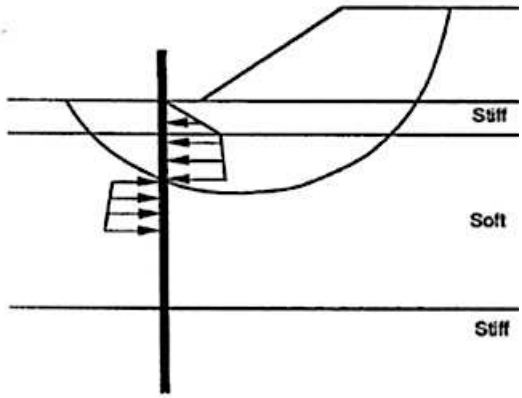

Figure 7. Approach according to De Beer & Wallays (1972) for h < 1.6

Tschebotarioff (1973) developed a recommendation, also based on a load by an embankment on a soft layer with a triangular load figure.

Broms (1976), on the other hand, developed a load-independent loading approach. Depending on the relative displacement $\bar{y}$ between the pile and the ground, the load is defined by a bedding modulus k. The bedding modulus is calculated by the magnitude of the undrained shear strength $c_{u,k}$ in relation to the pile width b.

$$p_{f,k} = k \cdot \bar{y} = \frac{10 \cdot c_{u,k}}{b} \cdot \bar{y} \quad (5)$$

In the case of non-cohesive soils, this approach cannot be applied due to the missing of flow pressure.

Due to the unequal compressibility of the different soil layers, the calculation model according to Powroschnik (1992) divides the pile into four load areas. With the direction of the relative displacements $\bar{y}$, actions and resistances change, which are defined as contact pressures with different signs. If the settlement of the soil is greater than the deflection of the inclined pile, an additional load pressure is applied over 3 times the flange width. In the case of cohesive layers, a corresponding flow pressure may be applied. If the pile comes into contact with the ground as a result of its deflection on its underside, the relative displacements $\bar{y}$ are directed upwards.

The approach of Kobarg (2001) is based on a static model that is simply partially clamped in the load-bearing ground and hinged at the head. The corresponding moment line is described by a sinusoidal curvature approach. The superposition with an original line of the same sign leads to a partial stress in the load-bearing soil.

3.3 *Comparison of existing models*

The calculation methods shown are based on different model concepts. Therefore, a calculation comparison is carried out at this point on the basis of a simply back-anchored quay wall cross-section.

The comparison of the common calculation methods explained shows a relatively good agreement in the determination of the maximum moment load in the field and clamping range. However, due to the unusual load figure and the calculation approach via an onload stress, very different curves of bending moments with a lower field moment result.

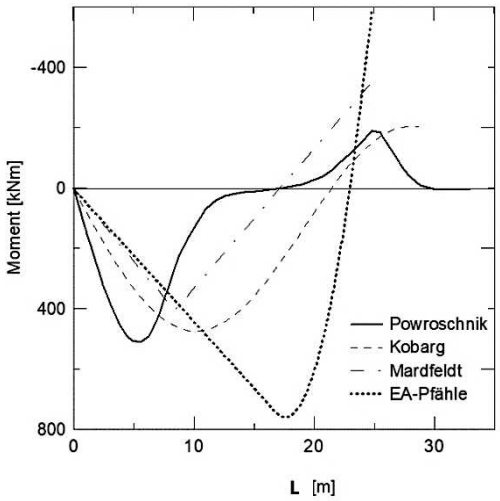

Figure 8. Comparison of different calculation approaches

The well-known calculation models described lead to very different results, which do not adequately reflect the measured cross-sectional variables. This is due on the one hand to the calculation approaches developed on the basis of static replacement models, but also to the very complex influencing variables of the real system, which make modelling difficult.

4 NEW CALCULATION APPROACH

Due to the complex boundary conditions the idea of implementing an universal bending formula approach seems to be ideal. The results of FEM parameter studies in particular show that the bedding and load stresses are very divergent and nonlinear (Höhmann 2010). The approach of calculating against a static determinate system is therefore inexpedient. However, with regard to the formation of plastic joints and the interaction with the normal force, a calculation based on a cutting variable seems inexpedient as well.

A description of the known deflection curves from inclinometer measurements seems more suitable. Based on this, the distribution of bending moments can be determined by differentiating twice.

The result of measurements in different construction projects is that the point of maximum deflection is in the range between 0.25*L and 0.35*L (Höhmann 2010). The ideal length L goes from the anchor head to the zero point of deflection in the area of the load-bearing soils, which represents a horizontal tangent there.

The member deformation can be described in a simplified way by superimposing a sinusoidal attachment with a parabola.

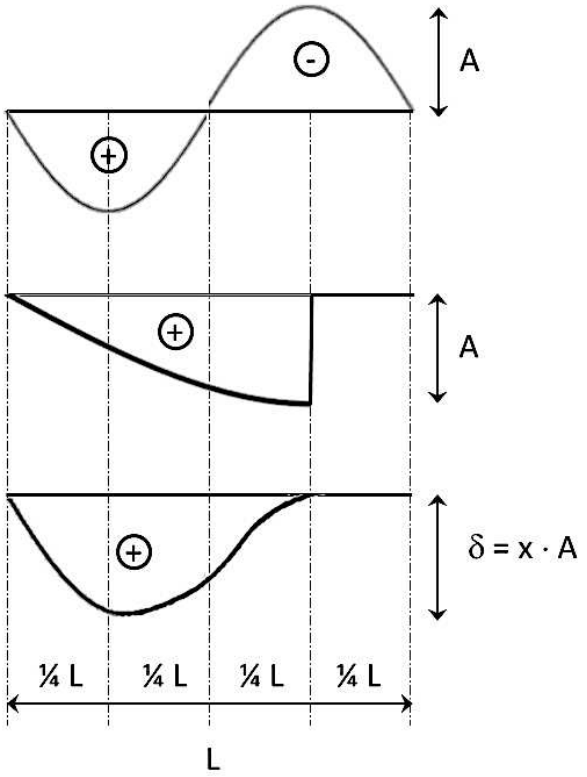

Figure 9. Sine and parabolic insertion and their superposition curve

The above sine function (Figure 8) can be described as follows:

$$z(x) = A \cdot \sin\left(\frac{2\pi}{l} \cdot x\right) \tag{6}$$

The quadratic parabola is described using a polynomial approach:

$$z(x) = a_0 + a_1 \cdot x + a_2 \cdot x^2 \tag{7}$$

By inserting the boundary conditions and forming, the solution of the polynomic approach is obtained. If you now superimpose the two approaches, you get a superposition curve. At the clamping point, the tangent runs horizontally and reflects the deflection of a driven inclined pile well.

$$z_{(x)} = A \cdot \left[\sin\left(\frac{2\pi}{l} \cdot x\right) + \frac{2x}{3/4\,l} - \frac{x^2}{\left(3/4\,l\right)^2}\right] \tag{8}$$

The maximum deflection (is 1.592*A) is about 0.29*l and is therefore within the range of the known measurements.

The curvature required to determine the moments is obtained via the 2-fold derivative:

$$z''_{(x)} = -A \cdot \left[\left(\frac{2\pi}{l}\right)^2 \cdot \sin\left(\frac{2\pi}{l} \cdot x\right) + \frac{2}{\left(3/4\,l\right)^2}\right] \tag{9}$$

5 CURVATURE DETERMINATION VIA DEFORMATION MEASUREMENTS

5.1 *General*

Inclinometer measurements of transversely loaded inclined piles show that the deflection curve of cannot be clearly described. It is only possible to numerically determine the distribution of bending moments from the inclinometer measurements with the help of difference quotients (Höhmann & Leible 2014).

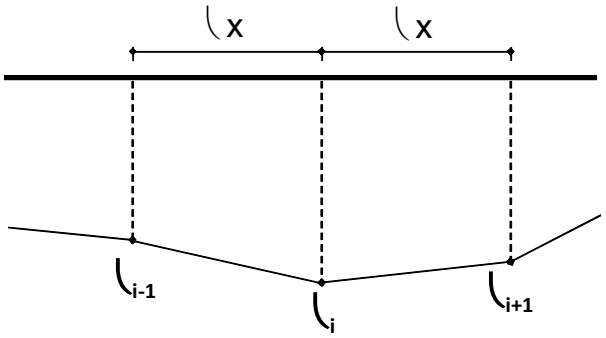

Figure 10. Evaluation methodology of deformations δi determined by inclinometer measurements with the measuring distance Δx for the application of the difference method

Deformation curves from inclinometer measurements represent a traverse of measuring points at a distance Δx of usually 0.5 or 1.0 m. With the help of the data, the curvature can now be determined numerically over a section of three measuring points (Fig. 9). For this purpose, the first and second derivatives of the function of the bending line are approximately replaced by difference quotients.

The change in deflection $w'(x)$ over the length Δx can then be determined as follows :

$$w'(x) = \frac{\Delta\delta_i}{\Delta x} = \frac{\delta_i - \delta_{i-1}}{\Delta x} \tag{10}$$

The curvature is thus obtained by deriving the deflection of three adjacent measuring points to:

$$w''(x) = \frac{\Delta^2\delta_i}{\Delta x^2} = \frac{\Delta\delta_{i+1} - 2\delta_i + \Delta\delta_{i-1}}{\Delta x^2} \tag{11}$$

With the help of the curvature curve determined from the bending line using the difference method, the moment along the length of the pile can be determined using Euler-Bernoulli Beam theory.

According to Marte (1998), measurement results are not unambiguous, but scattering variables that depend on the quantity to be measured and the measuring device. The inclinometer measurements shown in this thesis do not show a smooth curve, but have a slightly scattering curve due to the measurement errors, which can also be described as interference.

Therefore, an attempt is made to smooth out the measured data by means of a higher order polynomial and then to determine the bending curve using the dif-

ference equation method. This approach has the advantage that no boundary or storage conditions have to be specified. Only the fixing moment cannot be determined exactly. However, it can usually be assumed that the bearing is articulated, so that the moment at the beginning of the rod results in zero.

The deflection of an inclined pile over the smoothed and unsmoothed bending line of the inclinometer measurement data is an example of the deflection of an inclined pile investigated by inclinometer measurements.

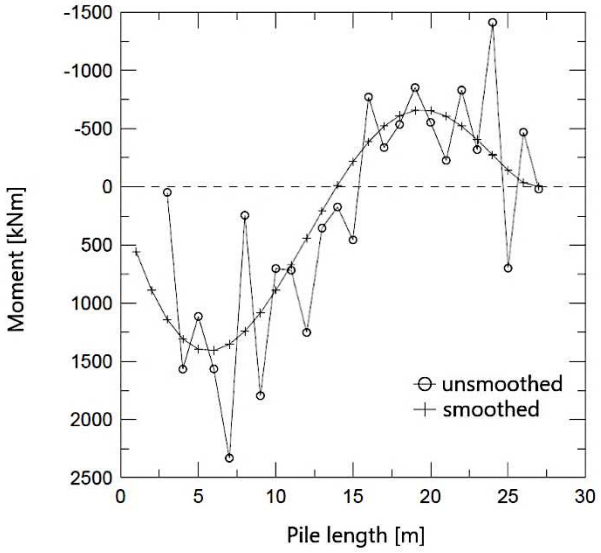

Figure 11. Determination of the moment loading from smoothed and unsmoothed inclination measurement data on a profile HTM 600/136 (S355)

It can be seen that the moment load on an inclined pile type HTM 600/136 (steel grade S355) determined from the backward calculation of inclinometer measurements must have been approximately M = 1400 kNm. The elastic moment bearing capacity would theoretically be far exceeded. However, with regard to the plasticizing capacity of the steel grade in question, these higher stress states can easily be plasticized out and thus have no negative influence on the limit load-bearing capacity.

6 CONCLUSIONS

In the present report, the problem of settling stressed inclined piles was shown. The causes of the influencing settlements can be different. Consolidation processes and compaction settlements are the significant influences on the deflection of inclined piles. Existing computational approaches based on elasticity theory show weaknesses in modelling in view of the available results of inclinometer settlements. Therefore, a verification method based on plasticity theory is recommended, as the elongation capacity of conventional structural steels is very large.

REFERENCES

Broms, B. 1976. Failure of pile-supported structures caused by settlements. *Proc. 6th European conf. Soil mech found. Eng* Wien.

De Beer, E.E. 1972. Forces induced in pile by asymetrical surcharges on the soil around the piles. *Proc. 5th European conf. Soil mech found. Eng* Madrid 1972, 1: 325-332.

De Beer, E.E. & Wallays, M. 1972. Forces induced in piles by unsymmetrical surcharges on the soil around the piles. *Proc. 5th ECSMFE* Madrid 1: 325-332

EA-Pfähle. 2013. *Recommendations on Piling (EA Pfähle). German Geotechnical Society (DGGT)*. Berlin: Wiley.

EAU. 2020. *Recommendations of the Committee for Waterfront Structures Harbours and Waterways, German Geotechnical Society (DGGT)*. Berlin: Wiley.

Höhmann, S. 2010. *Setzungsinduzierte Schrägpfahlbiegung, Industrial research report*. Bilfinger Berger AG.

Höhmann, S. & Leible, C. 2014. *Weiterentwicklung von Messsystemen im Spezialtiefbau und ihre Auswertemethodik, Conference for Geotechnical Measurements*. TU Braunschweig.

Smoltczyk, U. 2002. *Geotechnical Engineering Handbook. Volume 1*. Berlin: Ernst & Sohn.

Knappet, J. & Craig, R. 2020. *Craig's Soil Mechanics*. CRC Press, Taylor & Francis Group

Kobarg, J. 2001. Setzungsinduzierte Beanspruchungen von Schrägpfählen. *Bauingenieur* 76. Springer Verlag

Powroschnik, L. 1993. *Berechnung der Setzungsbiegung von Schrägpfählen*. Dissertation: Institute for soil mechanics, TU Darmstadt.

Tschebotarioff, G.P. 1973. *Foundations, retaining and earth structures* (2nd Edition). McGraw-Hill.

Terzaghi, K. 1943. *Theoretical soil mechanics*. New York: Wiley